



Trace and Rare Earth Elements Petrochemical Constraint on Tectonogenetic Evolution of the Granitoids of Zing-Monkin area, Adamawa Massif, N.E. Nigeria

Haruna I.V.¹, Orazulike D.M.² and Samaila N.K.²

¹Geology Department, Federal University of Technology, Yola, NIGERIA

²Geology Programme, Abubakar Tafawa Balewa University, Bauchi, NIGERIA

Available online at: www.isca.in

Received 24th August 2012, revised 5th September 2012, accepted 11th October 2012

Abstract

Zing-Monkin area is underlain by moderately radioactive biotite-hornblende-granodiorite, migmatites, equigranular granites, porphyritic granites, and highly radioactive fine-grained granite with subordinate pegmatites. Trace element contents of the granitoids decrease from granodiorite to the granites except Rb which behave in an opposite way. This results in a chemical gradient from granodiorite through the migmatites to the granites. The chondrite normalised rare earth elements trends indicate strongly fractionated rare earth element patterns with enriched light rare earth elements and an increasing negative Eu anomaly from the granodiorite to the granites. The gradational trace elements petrochemistry of the rock units and the antipathetic relation between Sr and Rb., Ba and Rb/Sr suggest that the granitoids are probably I-type, genetically related to a common source by fractional crystallisation. The within plate syn- to late-orogenic signatures suggest that the rocks were generated in a syn- to late-orogenic within plate tectonic setting.

Keywords: Granitoids, adamawa massif, petrochemistry, tectonic setting.

Introduction

Nigeria is situated within the Pan African mobile belt and sandwiched between the West African Craton to the west, the Taureq shield to the north and the Congo craton to the southeast (figure 1). Opinions are divided concerning the evolution of the Nigerian Pan African terrain. The first and most popular opinion is that the Nigerian Pan African terrain is the result of tectonic processes involving continental collision between West African craton and the Pan African mobile belt¹⁻⁵. The resultant heat, deformation and partial melting of the upper mantle and lower crust led to the emplacement of the granites. This interpretation is based on the observation of a suture along the eastern margin of the West African craton. The second opinion suggests that the Pan African orogeny was more of aggregation of crustal blocks such as island arcs and older continental fragments than a simple collision between two entities – the West African Craton and the Pan African⁶⁻⁹. The interpretation is based on the close association of calc-alkaline volcanics, ultramafic and basic rocks with the two major NE-SW trending fracture systems established in the western part of Nigeria.

Even though the former opinion has been widely accepted, some workers^{10,11} have observed that the Pan-African granites which extend to Nigeria and Cameroon, a distance of over 1500km from the suture cannot be related to the same subduction zone.

This paper uses trace and rare earth elements petrochemical data to enlarge information on geotectonic evolution of the basement rocks of North-eastern Nigeria.

Geological Setting: Zing-Monkin area is dominated by porphyritic granites and granodiorites (figure 2). Other rock units include migmatites, equigranular granites, and fine-grained granites, with pegmatites as the only minor rock unit. These rock form prominent rocky hills in the study area and exhibit considerable variation in texture and contact relationships.

The granodiorite occurs as inselbergs north of Wuro Alkali and occasionally as marginal masses of larger fairly porphyritic granodiorite bodies around Kobon Tolegbeng in the southern part of the area. In the eastern part of the area the rock occurs as sub circular to large elongate plutonic bodies spanning some kilometers. Though widely distributed in the eastern part of the area, individual occurrences of granodiorite are small except in the northeastern and southeastern parts where they occur as large elongate bodies.

Migmatite is of restricted occurrence in the area, occurring in a country between Yakoko and Monkin. A tract of country north of Ladana extending westward through Bansi to Honlipa and beyond is underlain by migmatite. At a bridge south of Busabore, the migmatite is well exposed and best studied at this locality.

Small subcircular stocks of equigranular granite run from north to south along the western border of the study area. The southern hills of kozin are formed by equigranular granite. The most important development of equigranular granite occurs north of Danyo where they form rugged hills. The greater part of the hilly country at kobon Nyapali is formed by this rock unit.

Widespread and extensive development of porphyritic granite occurs throughout the study area. The greater part of the hilly country between Mapo and korako, the country north of Yakoko, the southwestern part of Monkin and the hills southwest of Danyo are underlain by porphyritic granites.

Fine-grained granite, like the migmatite, is of subordinate occurrence in the study area. It occurs only in two locations: around Nmadi and at kozin. At Nmadi the rock occurs as low

lying intrusive body with numerous fractures. At kozin it is found cross cutting the host equigranular granite.

Pegmatite do not form independent or mappable rock units in the study area except at a locality southwest of Danyo where they form a small hill of rock consisting of graphic intergrowth of quartz and potash feldspars. At this locality, the rock takes the form of quartz-feldspar body a few tens of meters in length.

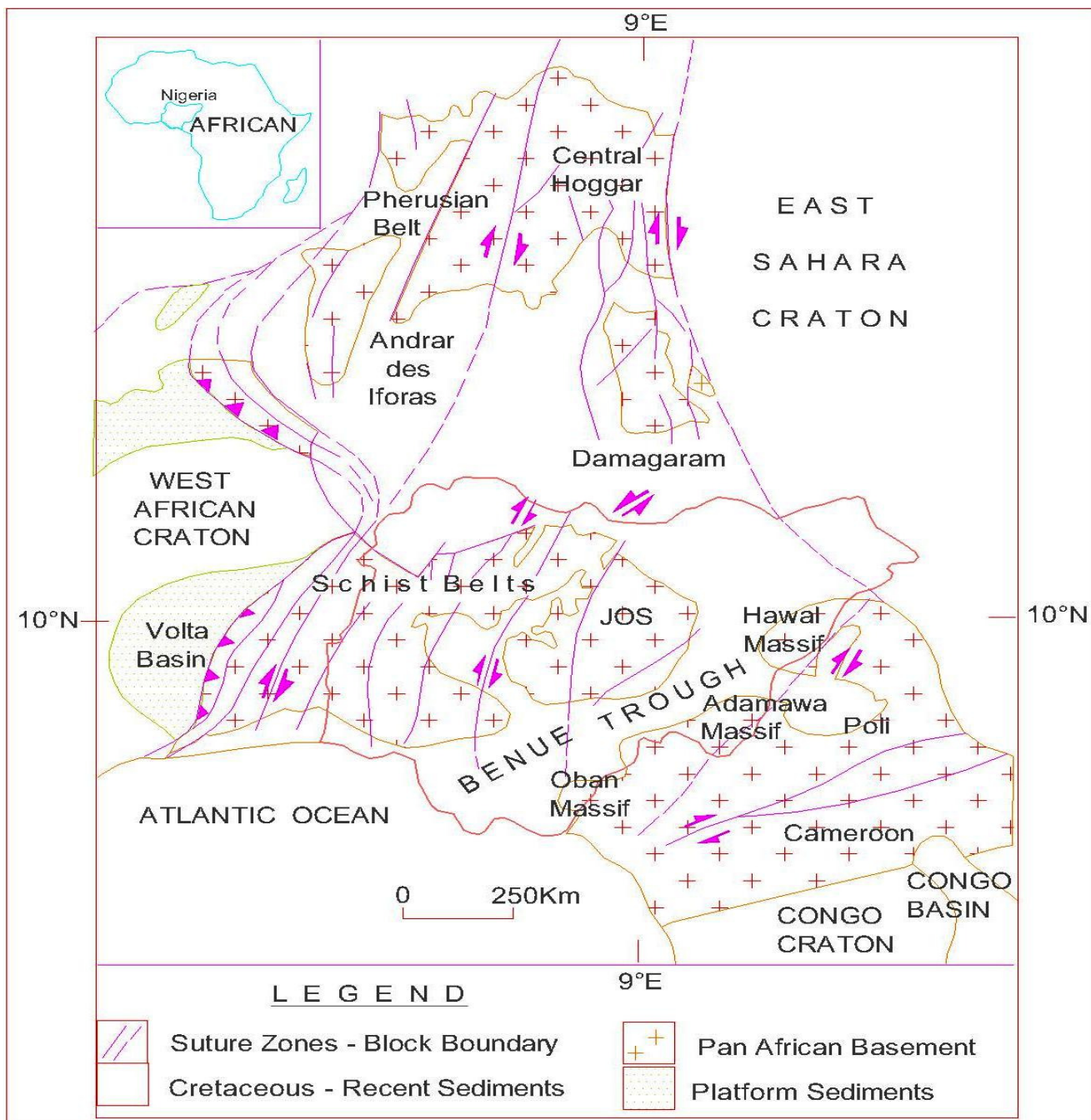


Figure-1
 Regional Geological setting of Nigeria (modified after Ferre et al., 1996)

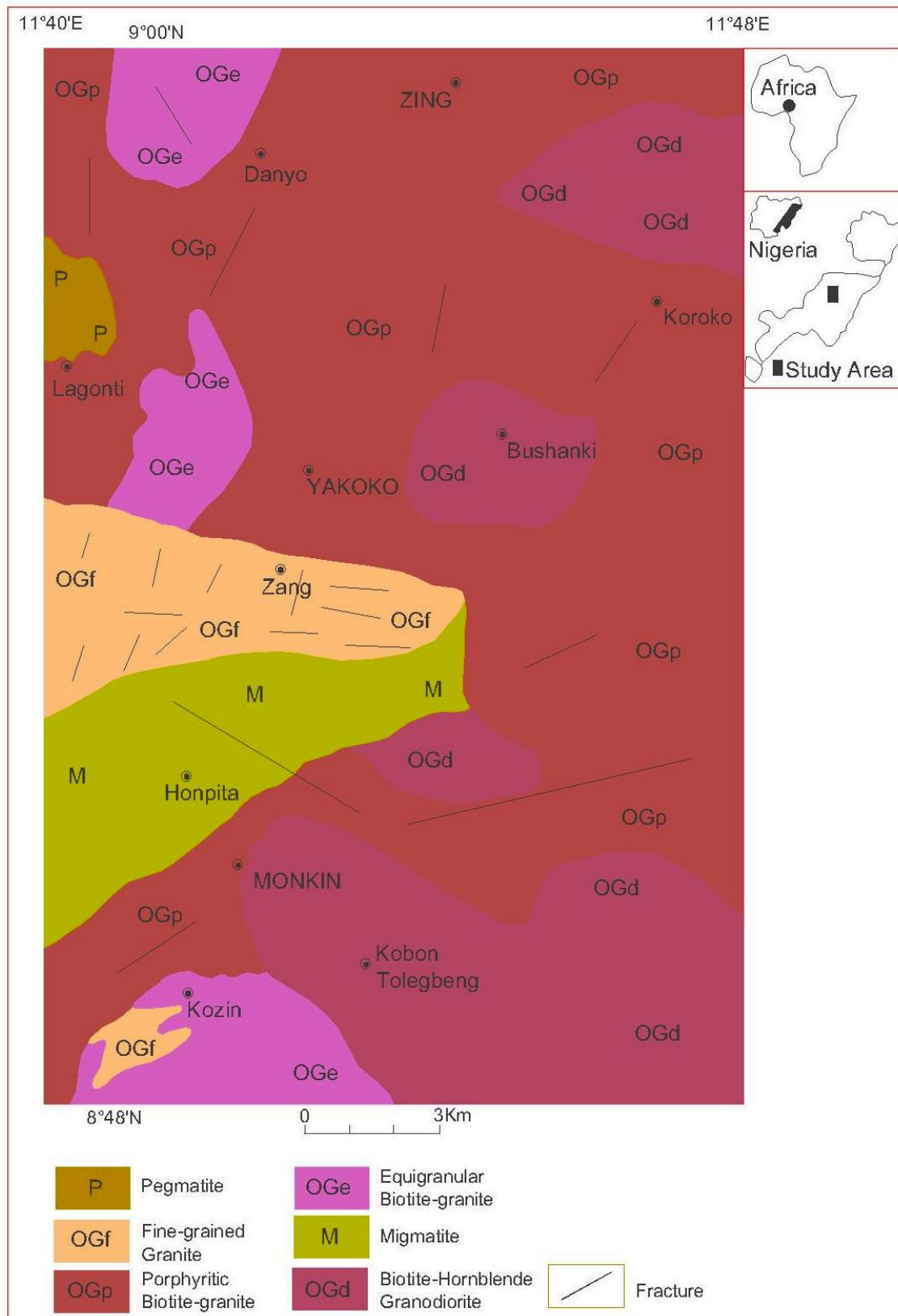


Figure-2
 Geology of Zing-Monkin area (present work)

Material and Methods

Analytical Procedure: Petrochemical analyses of carefully selected representative rock samples from different rock units were carried out in the Activation Laboratory, Canada. Total digestion employing hydrochloric, nitric, perchloric and hydrofluoric acids dissolves most silicates. However refractory minerals particularly zircon, sphene, magnetite, monazite, chromite, and several other phases may not be totally dissolved. If these minerals are not digested a bias may occur for certain REE and HFSE with acid digestion. Consequently aggressive fusion technique employing lithium metaborate/tetraborate fusion was chosen for the analyses. The resultant molten bead is rapidly digested in a weak nitric acid solution. The fusion ensures that the entire sample is dissolved. It is only with this attack that trace elements and REE are put into solution. The dissolved samples were analysed for trace and rare earth elements using fusion ICP/MS package. Precision of analytical data was monitored by international rock standard. Such precision for trace elements is better than 5%.

Results and Discussion

Trace Elements: The result of trace element analysis is presented in table 1. The number of trace elements analysed are far more than the number required for this study. Therefore only those which have direct implication to petrogenesis are discussed in this study. The table shows a systematic decrease in Ba, Sr and Zr from the granodiorite through migmatites and equigranular granite to fine-grained granites. In contrast, Rb, Th and Rb/Sr ratio increase steadily from granodiorite through equigranular and porphyritic granites to fine-grained granites. Both the concentrations and patterns of the trace elements are significantly different from those found in sediments¹²⁻¹⁵, soil¹⁶, and water¹⁷⁻¹⁹.

Table-1
 Trace elements petrochemical (ppm) data for the for the granitoids of Zing-Monkin area

Sample#→	1	2	3	4	5	6	7	8	9	10	11	12	13	14	15
Sc	11	12	16	7	4	3	3	2	4	6	3	1	3	3	3
Be	12	11	3	2	3	2	3	6	4	2	4	3	3	3	3
V	61	70	68	14	22	40	<5	<5	5	10	<5	21	5	9	6
Ba	1590	1254	1073	1012	786	1832	393	22	444	1078	36	1333	465	464	472
Sr	495	479	251	164	233	685	96	11	106	172	17	440	126	131	130
Y	33	33	63	62	27	11	24	45	98	47	22	13	14	18	32
Zr	213	268	569	480	266	297	293	67	196	393	49	136	129	140	123
Cr	<20	<20	<20	<20	<20	<20	<20	<20	<20	<20	<20	<20	<20	<20	<20
Co	17	14	23	13	15	15	14	18	17	16	18	19	11	14	15
Ni	<20	<20	<20	<20	<20	<20	<20	<20	<20	<20	<20	<20	<20	<20	<20
Cu	<10	<10	<10	<10	10	<10	<10	<10	<10	<10	<10	<10	<10	10	<10
Zn	70	90	140	60	50	60	40	<30	40	80	<30	<30	<30	40	30
Ga	27	27	27	27	26	22	21	29	24	25	23	21	20	20	21
Ge	1	1	2	2	1	<1	1	2	2	2	1	1	1	1	1
As	<5	<5	<5	<5	<5	<5	<5	<5	<5	<5	<5	<5	<5	<5	<5
Rb	234	250	175	250	224	158	210	368	310	230	290	206	286	294	299
Nb	22	23	34	30	15	12	11	42	24	26	16	8	15	14	15
Mo	<2	<2	<2	<2	<2	<2	3	<2	<2	<2	<2	<2	<2	<2	<2
Ag	<0.5	<0.5	<0.5	<0.5	<0.5	<0.5	<0.5	<0.5	<0.5	<0.5	<0.5	<0.5	<0.5	<0.5	<0.5
In	<0.2	<0.2	<0.2	<0.2	<0.2	<0.2	<0.2	<0.2	<0.2	<0.2	<0.2	<0.2	<0.2	<0.2	<0.2
Sn	4	5	5	3	3	4	3	2	7	4	3	4	5	5	5
Sb	<0.5	<0.5	<0.5	<0.5	<0.5	0.9	0.6	<0.5	<0.5	0.9	<0.5	<0.5	<0.5	1.5	<0.5
Cs	8.4	10.8	1.6	0.9	2.3	1.1	2.7	2.4	2.9	1.6	3.7	2.6	6	6.3	5.9
Hf	5.2	7.5	13.5	14.1	7.2	7.3	7.5	3.9	5.8	11.4	2.2	3.6	3.9	4.3	3.9
Ta	3.9	3.9	2.7	1.8	1.5	0.8	0.7	6.2	2.3	1.9	1.3	1.2	2	1.8	1.8
W	65	46	80	77	85	82	94	121	115	109	134	124	74	96	105
TI	1.2	1.8	1.2	1.4	1.3	1.6	1.8	1.7	1.7	1.8	2.1	1.2	2.2	3.1	2.3
Pb	15	22	17	22	18	42	25	36	26	34	42	22	32	49	32
Bi	<0.4	<0.4	<0.4	<0.4	<0.4	<0.4	<0.4	<0.4	<0.4	<0.4	<0.4	<0.4	<0.4	<0.4	<0.4
Th	12.5	14.5	28.6	61.3	37.8	25.2	35.9	15.3	56.6	45.7	27.5	30.8	28.9	37.4	47
U	2.6	2.4	2.2	2.6	3	2.4	2.4	8.6	5	2.3	5	1.6	4.6	4.9	5.3
Rb/Sr	0.47	0.52	0.70	1.52	0.96	0.23	2.19	33.5	2.92	1.34	17.1	0.47	2.27	2.24	2.3

Sample 1 – 3 = granodiorite; sample 4 – 6 = migmatite; sample 7 – 9 = equigranular granite; sample 10 – 12 = porphyritic granite; sample 13 – 15 = fine-grained granite.

A plot of Rb, Sr and Ba on a trivariate diagram (figure 3)²⁰ shows that the fine-grained granites are the most differentiated. Rb⁺ has larger radius than K⁺. Consequently, Rubidium is always admitted in to potassium minerals such as biotite and potassium minerals. Since potassium is the only major element Rubidium can replace, Rubidium concentration in the melt increases with differentiation. Strontium, on the other hand, can replace two major elements: calcium and potassium. It (strontium) can be admitted to calcium minerals (on account of its higher radius) or captured by potassium minerals (on account of its higher charge). Table 1 has shown that admittance in place of calcium is the dominant process of removal of strontium from the magma. Hence, with progressive crystallisation, strontium is systematically depleted in the melt. Barium cannot replace calcium or sodium because of its large radius (1.34Å). The only major element of comparable ionic size is potassium, and so, on account of its (barium) higher charge, barium is captured by potassium compounds. It therefore appears in biotite and potash feldspar. Thus crystallisation of these minerals contributes to reduction of barium in the melt. Zr on the other hand, is a classical incompatible element, not readily substituting in major mantle phases.

However, they may substitute for Ti in accessory phases such as sphene and rutile. This probably explains why Ti concentration increases with decreasing Zr values. Low Ni (<20ppm), Co (<24ppm), Cr (<20ppm) values rule out the possibility of a peridotite progenitor since high values of Ni (250ppm to 300ppm) and Cr (500ppm to 600ppm) are good indicators of parental magma from a peridotite mantle source.

Trace elements plotted against one another as proposed by some workers²¹⁻²³ can give indications into the covariation between elements, petrogenetic constraints and tectonic environment. On Rb versus (Yb+Ta)²¹ (figure 4a), all the samples plot in the field of ocean ridge granites. On the Rb versus (Yb+Nb) plot (figure 4b), the samples are almost equally divided between within-plate granite and ocean ridge granite fields. When Nb is plotted against Y in figure 4c, most of the samples show syn-collisional granite signatures with few in the within-plate granite group. This signature is also indicated in a plot of Ta versus Yb (figure 4d) in which the samples are divided between the fields of within-plate granite, syn-collisional granite and volcanic-arc granite.

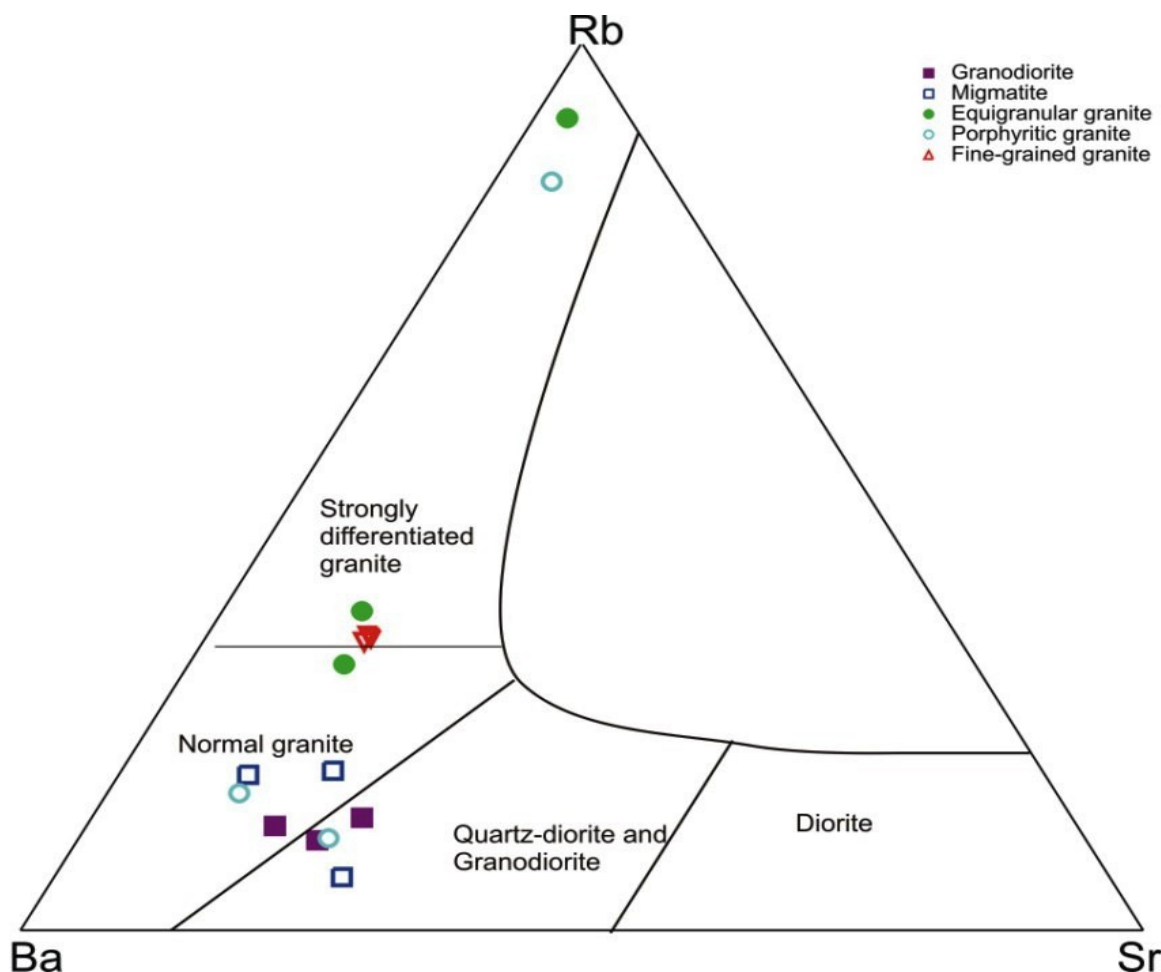


Figure-3

Rb, Sr and Ba variation plots plot for the granitoids of Zing-Monkin area (after El-Bouseily and El-Sokkary, 1975)

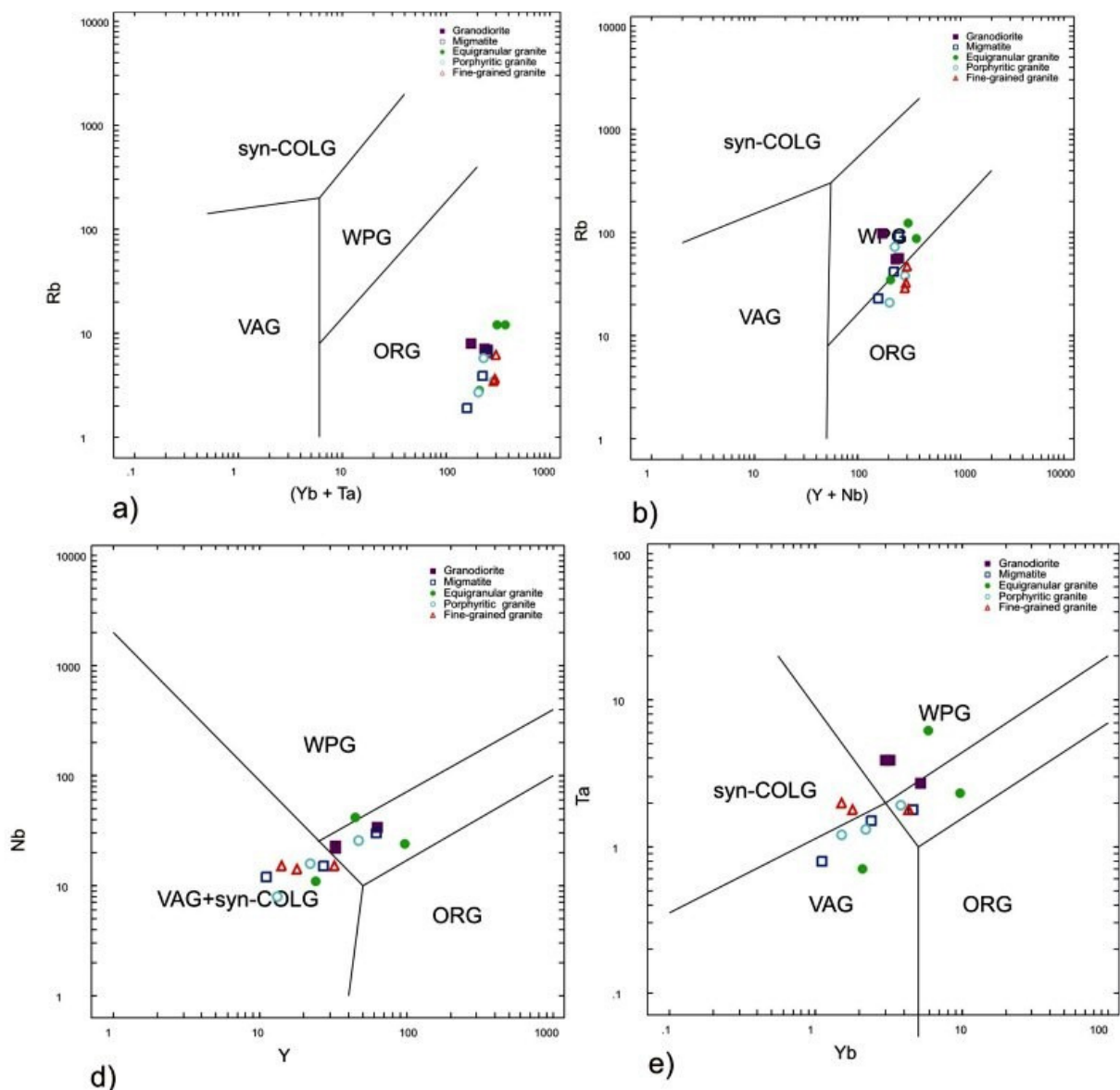


Figure-4

Tectonic plots for the granitoids of Zing-Monkin area (after Pearce et al., 1984). a) Rb Vs (Yb+Ta), b) Rb Vs (Y+Nb), c) Nb Vs Y, d) Ta Vs Yb

Rare Earth Elements (REE)

Result of REE data is presented in table 2. The table shows that the granitoids of the study area are generally more enriched in light REE than the heavy REE. The granitoids show considerable variation in their concentrations across the rock units with Oddo-Harkins effect clearly indicated in the data. Therefore, in order to compare the abundances of REE graphically, this effect has been eliminated through normalising the concentrations of individual REE to their abundances in chondritic meteorite as proposed by some authors^{24,25}. The REE distribution pattern varies slightly from one rock unit to another. The granodiorite (figure 5a) display fractionated REE patterns [(La/Yb)N = 10.59 on average] and exhibits slightly fractionated

LREE enriched pattern [(La/Sm)N = 2.87 on the average] and almost flat HREE [(Tb/Yb)N = 1.58 on the average] and very small negative Eu anomalies (Eu/Eu* = 0.69 on the average). Migmatite (figure 5b) exhibits stronger fractionated pattern [(La/Yb)N = 28.35 on the average] for REE and display a fairly strong LREE-enriched pattern [(La/Sm)N = 4.61 on the average] with a near flat HREE [(Tb/Yb)N = 1.88 on average] distribution pattern similar to granodiorite and has almost negligible negative Eu anomalies (Eu/Eu* = 0.50 on average). Equigranular granite (figure 5c) is characterised by relatively fractionated patterns [(La/Yb)N = 9.8 on average] with slightly enriched LREE distribution pattern [(La/Sm)N = 2.99 on average] and relatively flat HREE [(Tb/Yb)N = 1.22 on

average]. Unlike the granodiorite and migmatite, the equigranular granite displays large negative Eu anomalies ($Eu/Eu^* = 0.20$). REE abundances in porphyritic granite (figure 5d) are characterised by strongly fractionated patterns [(La/Yb)N = 15.46 on average] with a strongly fractionated LREE-enriched patterns [(La/Sm)N = 3.97 on the average]. It displays a near flat HREE pattern [(Tb/Yb)N = 1.44 on average] and exhibits small negative Eu anomalies ($Eu/Eu^* = 0.44$ on average). Fine-grained granite (figure 5e) exhibits fractionated REE patterns [(La/Yb)N = 13.57 on the average] and displays fairly strong fractionated LREE-enriched patterns [(La/Sm)N = 3.67 on average] with relatively flat HREE trends [(Tb/Yb)N = 1.48 on average] and appreciable negative Eu anomalies ($Eu/Eu^* = 0.28$ on average). A combined chondrite-normalised diagram (figure 5f) for the granitoids of the study area shows that the REE abundances are characterised by fractionated patterns [(La/Yb)N = 15.55 on average] and displays strongly fractionated LREE-enriched trends [(La/Sm)N = 3.62 on average] with less fractionated HREE patterns [(Tb/Yb)N = 1.52 on average] and significant negative Eu anomalies ($Eu/Eu^* = 0.41$ on average). Fine-grained granite and equigranular granite have much lower average REE content (TotREE = 223.86 and 275.07 respectively) relative to porphyritic granite and granodiorite (TotREE = 322.13 and 345.70 respectively). Migmatite has the highest REE content (TotREE = 492.66). The combined REE distributions patterns are emphasised in figure 5g. A spider plot of the REE values normalised to average continental crust (figure 5h)²⁶ shows depletion in the contents of Ba, Sr, P and Ti.

The total concentrations of the elements decrease from granodiorite through migmatite to the more evolved granites indicating a negative correlation between rare earth elements concentration and acidity of the rocks. This may be a reflection of the role of garnet, hornblende, sphene, and plagioclase in fractionation processes. Sphene has the effect of accommodating the light REE. These light rare earth elements are strongly fractionated by garnet and hornblende which readily accommodate the heavy rare earth elements. Eu is strongly fractionated into feldspars and Eu anomalies may reflect feldspar involvement in the fractionation process.

Petrogenetic constraints: Mantle and crust are the two end member sources of granitoids. However, the two sources are not mutually exclusive. While most granitic rocks originate by contribution from both sources, some are derived purely from the end member sources^{27,28}. The composition of the source and the physico-chemical processes that affect this source and the melt therefore control the chemistry of granitic rocks. The relatively uniform composition of the granitoids and overlapping ranges in most of their trace and rare earth element abundances suggest that the rocks are derived from a similar parental magma source. This genetic relationship between the granodiorite and the granites is clearly evident in the smooth chemical gradient from granodiorite to the granites. The slight differences in some of the trace elements abundances and REE trends of the rock units may be explained by their different evolutionary histories.

Table-2
Rare Earth Elements (ppm) petrochemical data for the granitoids of Zing-Monkin area

Sample#→	1	2	3	4	5	6	7	8	9	10	11	12	13	14	15
La	49.3	51.6	103	203	86.7	66.1	82	8.1	78.5	185	4.6	38.6	40.4	48.2	57.8
Ce	114	122	228	411	140	130	168	11.9	176	368	9.7	72.9	87.3	99.5	120
Pr	13.3	13.1	25.9	44.5	17.1	13.8	17.8	2.05	19.4	38.4	1.37	6.86	9.15	10.9	12.4
Nd	44.8	48.3	89.1	143	53.3	39.5	54.7	10.9	65.2	122	7.9	20	30.1	36.8	43.8
Sm	9.4	10.6	18.4	29	10.4	6.7	9.9	3.5	13.6	21.9	2.9	3.3	6	7.2	8.7
Eu	1.95	2.12	2.82	2.21	1.32	1.42	0.85	0.13	0.84	2.31	0.16	0.76	0.56	0.59	0.6
Gd	7.7	7.6	15	18.7	7.2	3.6	6.7	5.3	12.6	13.8	3.3	2.6	3.9	4.9	6.7
Tb	1.1	1.1	2.1	2.5	1	0.4	0.9	1.2	2.2	1.8	0.6	0.4	0.6	0.7	1.1
Dy	5.6	6	11	13.2	5.1	2	4.9	8.4	13.2	9.4	4.1	2	3	3.7	6.4
Ho	1.1	1.2	2.1	2.4	1	0.4	0.9	1.9	2.9	1.8	0.8	0.4	0.5	0.7	1.4
Er	3.3	3.4	6.3	6.6	3.1	1.1	2.4	5.8	9.6	5.1	2.5	1.3	1.6	1.9	4.5
Tm	0.52	0.5	0.88	0.87	0.44	0.16	0.34	0.93	1.53	0.68	0.37	0.22	0.24	0.27	0.69
Yb	3.2	3	5.2	4.6	2.4	1.1	2.1	5.9	9.7	3.8	2.2	1.5	1.5	1.8	4.3
TotREE	255.7	270.9	510.5	882.2	329.37	266.4	351.8	66.85	406.6	774.5	40.82	151.1	185.1	217.5	269.0
Lu	0.41	0.42	0.69	0.6	0.31	0.16	0.29	0.84	1.3	0.52	0.32	0.21	0.25	0.29	0.65
(Tb/Yb)N	1.46	1.56	1.72	2.31	1.77	1.55	1.82	0.87	0.97	2.02	1.16	1.13	1.70	1.65	1.09
(La/Yb)N	9.34	10.42	12.00	26.75	21.89	36.42	23.67	0.83	4.90	29.51	1.27	15.60	16.32	16.23	8.15
(La/Sm)N	2.88	2.67	3.07	3.84	4.57	5.41	4.54	1.27	3.17	4.63	0.87	6.42	3.69	3.67	3.64
Eu/Eu*	0.68	0.69	0.50	0.27	0.44	0.80	0.30	0.09	0.19	0.38	0.16	0.77	0.33	0.29	0.23

Sample 1 – 3 = granodiorite; sample 4 – 6 = migmatite; sample 7 – 9 = equigranular granite; sample 10 – 12 = porphyritic granite; sample 13 – 15 = fine-grained granite.

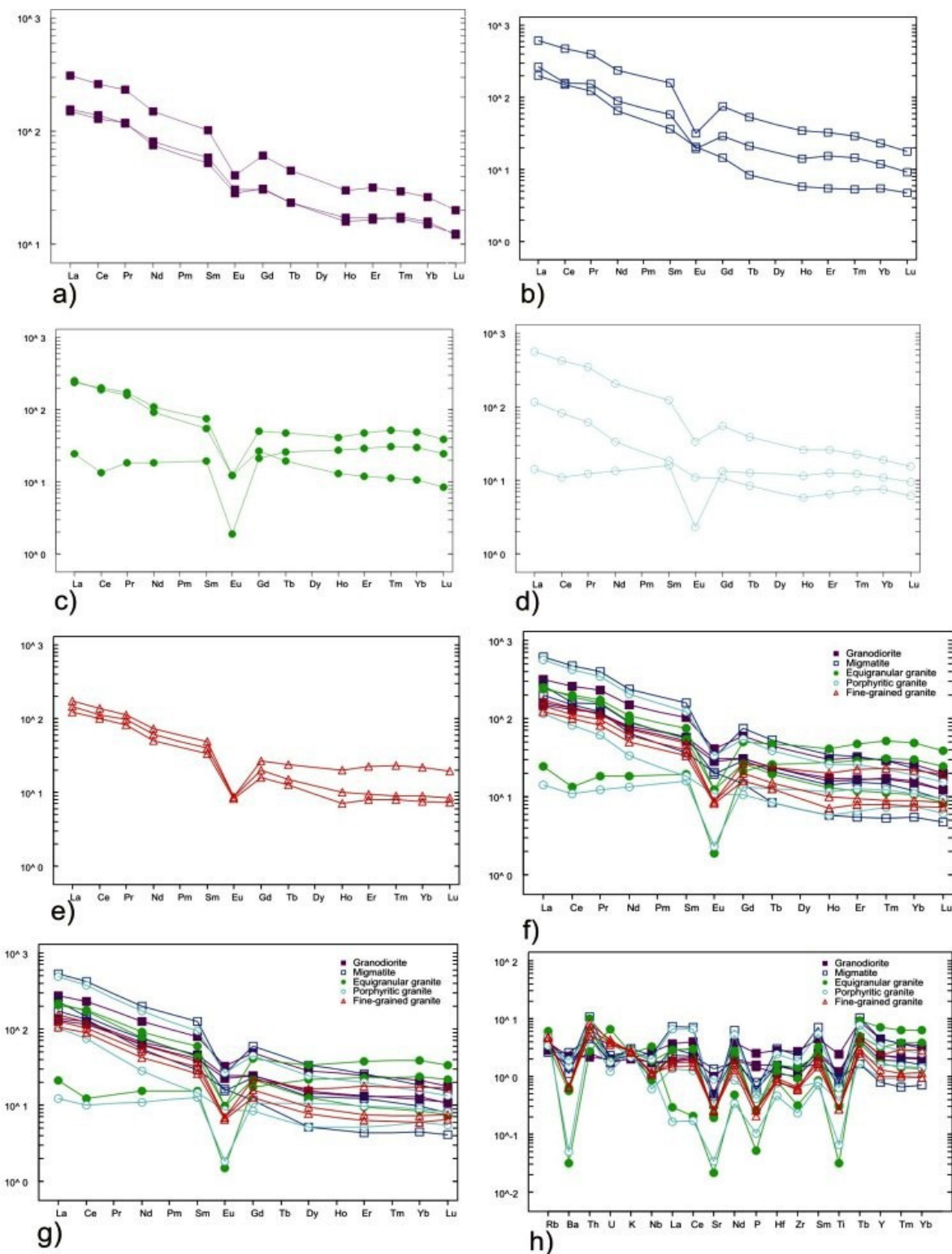


Figure-5

Chondrite-normalised (normalising values of Hasken et al., 1968) REE abundances for (a) granodiorite, (b) migmatite, (c) equigranular granite, (d) porphyritic granite and (e) fine-grained granite. Combined chondrite-normalised REE abundances for the granitoids of Zing-Monkin area using the normalising values of (f) Hasken et al (1968), (g) Masuda et al., (1973). (h) Spider diagram for the granitoids normalised to average continental crust according to Weaver and Tarney, (1984)

The Granodiorite: The fairly high values of Rb, Ba and LREE and Rb/Sr ratios suggest that the granodiorite belongs to the I-type granitoids probably derived by partial melting of a basic source²⁹. Fractionation of basic melts to yield silicic magmas is normally dominated by the removal of plagioclase to produce significant negative Eu anomalies. The near absence of Eu anomalies in the granodiorite ($Eu/Eu^* = 0.63$) is inconsistent with this concept. Enrichment of Ba, and Rb contents in the granodiorite precludes its formation by melting of possible surrounding greywackes as liquids generated from melting of greywackes is often depleted in these elements³⁰. Furthermore, melts derived from granulitic residue in the lower continental crust is generally depleted in LILE. Thus, the high content of LILE (e.g Sr, Ba, Zr) in the investigated granodiorite argues against its formation from such melts. According to some authors^{31,32}, rocks with LREE-enriched patterns and characterised by negligible Eu anomalies (similar to Zing-Monkin granitoids) are compatible with generation by partial melting from basic source in which amphibole and/or garnet are present as residual phases in the source. Negligible Eu anomalies and fractionated REE patterns of the granodiorite are in agreement with the control of amphibole with minor plagioclase crystallisation³². Similarly, high LREE/HREE ratios of the granodiorite are common with the presence of amphibole as residual phase during partial melting. The partial melting model for the granodiorite is further supported by the high contents of V, Nb, Zr, Yb, and Y. This is because the low contents of these elements would have suggested that fractionation of amphibole, minor biotite and accessory phases significantly contributed to the chemical evolution of the rocks. However, the fact that there is Eu anomalies (though negligible) shows that there is minor contribution from fractionation processes.

Field characteristics of the granodiorite such as the presence of mafic enclaves (earlier identified in the field) may be suggestive that the granodiorite was generated by partial melting of basaltic source^{30,33}. The mafic enclaves can be interpreted as refractory residues (restites) occurring after high degrees of partial melting of a basaltic source.

The Granites: The granites show pronounced negative Eu anomalies, and lower Sr, Ba and Eu. These elements reflect plagioclase retention as a residual phase in the melt. Petrochemical modelling of Rb and Sr during melting suggests that a fluid present melting reaction of muscovite + plagioclase + quartz would produce melts with average Rb/Sr ratios of <1.50 ³⁴. The granites have higher average Rb/Sr ratios than the granodiorite. The high Rb/Sr ratios in the granites suggest that any fluid present during their formation must have low H₂O content. Such Rb/Sr ratios may nevertheless suggests that the granites are residual from the granodiorite after fractionation of hornblende, biotite and minor plagioclase as indicated by the near absence of Eu anomalies in the granodiorite. All these evidences suggest fractional crystallisation as the dominant process in the formation of the granites. Generally, the REE

abundance trends reflect the residual mineral assemblages of their source regions. The REE abundance patterns of the granites are in consonance with fractionation of plagioclase and biotite. The decrease in the LREE content of the granites may be explained by the role played by the REE-bearing accessory minerals such as apatite, zircon, and allanite³⁵.

The granites, particularly the fine-grained granites show REE trends, characteristic of highly differentiated granites and an almost flat LREE-HREE abundance patterns with significant negative Eu anomalies ($Eu/Eu^* = 0.28$). These REE abundance trends suggest that the granites (especially the fine-grained granites) are more differentiated and can be accounted for by fractional crystallisation model. Eu anomaly suggests plagioclase fractionation or retention of refractory plagioclase, and the decreased LREE content with differentiation may be explained by accessory phases (e.g apatite, zircon, rutile, ilmenite, sphene, allanite) which are common accessories in granites. The slight increase in HREE (from granodiorite to granites) during differentiation can be accounted for by the combined effects of feldspar, quartz and biotite fractionation, which would increase all the REE in the residual melt, and accessories fractionation which preferentially removes the LREE and enriches in HREE³⁶.

Tectonic Environment: Methodical trace element variation plots encompassing granites from practically all possible tectonic environments have been developed by several workers²¹⁻²³. According to those workers, granites can be discriminated on the basis of Nb, Y, Ta, Yb, and Rb trace element data into volcanic-arc, ocean ridge, within-plate and collisional (syn- and post-collisional) types. On the Rb Vs ($Yb+Ta$)²¹, all the rock units plot within the ORG field. When Rb is plotted against Y+Nb, the granitoids are divided between the WPG and ORG regions. On Nb Vs Y and Ta Vs Yb²¹, samples from granodiorite and equigranular granite plot mainly within the WPG field while samples from migmatite, porphyritic granite and fine-grained granite plot within the VAG and syn-COLG fields. All the rock units have average Y/Nb ratios greater than 1.2 which correspond to I-type granites generated in a subduction related environment³⁷. This is fairly consistent with aforementioned classification and shows that the granitoids were emplaced in a syn- to late-orogenic tectonic environment. Also, since the granitoids have WPG signatures in most of the diagrams with only minor VAG and ORG affinities, it can be said that the granitoids were emplaced in within plate tectonic environment. Collectively, the diagrams suggest that the granitoids of Zing-Monkin area were emplaced in a syn- to late-collisional within plate tectonic setting.

Conclusion

On the basis of trace and rare earth elements petrochemical characteristics presented in this work, the granitoids are I-type generated in a syn- to late-orogenic within plate tectonic setting. The granodiorite and granites are genetically related to a

common source. The granodiorite were most likely formed by partial melting of a basic source. Subsequent fractionation of hornblende, plagioclase and biotite in an orogenic environment led to the production of the granites.

References

1. Burke K.C. and Dewey F.J., Orogeny in Africa, In: T.F.J. Dessauvage and A.J. Whiteman (Editors) African Geology, Geology Department, Univ. Ibadan, Nigeria, 583-608 (1972)
2. Bertrand I.M.L. and Caby Y.R., Geodynamic evolution of the Pan-African orogenic belt, A new interpretation of the Hoggar Shield (Algerian Sahara), *Geol. Rund.*, (67), 357-388 (1978)
3. Black R., Caby R., Pouchkine A., Bayer B., Bertrand J.M., Boullier A.M., Fabre J. and Lesquer A., Evidence for Late Precambrian plate tectonics in West Africa, *Nature*, (278) 223-227 (1979)
4. Trumpette R., The Pan-African Dahomeyide fold belt: a collision orogeny? (Abstract), 10th colloque de Geologic Africaine, Montpellier, 72-73 (1979)
5. Caby Y.R., Bertrand J.M. and Black R., Pan African ocean closure and continental collision in the Hoggar-Iforas segment, Central Sahara, In: A Kroner (Editor) Precambrian plate Tectonics. Elsevier, Amsterdam, 407-434 (1981)
6. Wright J.B. and Ogezi A.E.O., Serpentinite in the Basement of Northwestern Nigeria, *Journ. Mining Geol.*, (14), 34-37 (1977)
7. McCurry P. and Wright J.B., Geochemistry of calc-alkaline volcanics in northwestern Nigeria, and a possible Pan-African suture zone, *Earth Planet. Sci. Lett.*, (37), 90-96 (1977)
8. Holt R.W., Egbuniwe I.G., Fitches W.R. and Wright J.B., The relationships between low grade metasedimentary belts, calc-alkaline volcanism and the Pan-African orogeny in NW Nigeria, *Geol. Rand.*, (67), 631-646 (1978)
9. Ajibade A.C., Woakes M. and Rahaman M.A., Proterozoic crustal development in the Pan-African regime of Nigeria. In: C.A. Kogbe (Ed) Geology of Nigeria 2nd Revised Edition. Elizabethan publication company, Lagos, 57-69 (1989)
10. Black R., Granite: From Segregation of Melt to Emplacement, *Episodes* (4), 3-8 (1980)
11. Turner D.C., Upper Proterozoic schist belts in the Nigerian sector of the Pan African province of West Africa, *Precamb. Res.*, (21), 55-79 (1983)
12. Nwajei G.E., Okwagi P., Nwajei R.I. and Obi-Iyeke G.E., Analytical Assessment of Trace Elements in Soils, Tomato Leaves and Fruits in the Vicinity of Paint Industry, Nigeria, *Res. J. Recent Sci.*, 1(4), 22-26 (2012)
13. Shama S., Naz I., Ali I. And Ahmed S., Monitoring of Physico-chemical and Microbiological analysis of Underground Water Samples of District Kallar Syeddan, Rawalpindi-Pakistan, *Res. J. Chem. Sci.*, 1(8), 24-30 (2011)
14. Parihar S.S., Ajit K., Ajay K., Gupta R.N., Manoj P., Archana S. and Pandey A.C., Physico-chemical and Microbiological Analysis of Underground Water in and around Gwalior City, MP, India, *Res. J. Recent Sci.*, 1(6) 62-65 (2012)
15. Iwuoha G.N., Osuji L.C. and Horsfall M. Jnr., Index Model Analysis Approach to Heavy Metal Pollution Assessment in Sediments of Nworie and Otaro, *Res. J. Chem. Sci.*, 2(8), 1-8 (2012)
16. Osakwe S.A., Chemical Partitioning of Iron, Cadmium, Nickel and Chromium in Contaminated Soils of South-Eastern Nigeria, *Res. J. Chem. Sci.*, 2(5), 1-9 (2012)
17. Ishaku J.M., Nur A. and Bulus J.A., Mapping of Groundwater Facies using anion Geochemistry in Angware Area, Jos Northcentral Nigeria, *Res. J. Chem. Sci.*, 2(6), 21-29 (2012)
18. Murhekar G.H., Assessment of Physico-Chemical Status of Groundwater Samples in Akot City, *Res. J. Chem. Sci.*, 1(4), 117-124 (2011)
19. Obiefuna G.I. and Orazulike D.M., The use of Anion Geochemistry in Mapping Groundwater Facies of Yola Area, NE Nigeria, *Res. J. Chem. Sci.*, 1(16), 30-41 (2011)
20. El-Bousely, A.M. and El-Sokkary, A.A., The relation between Rb, Ba and Sr in granitic rocks, *Chem. Geol.*, (16), 207-219 (1975)
21. Pearce J.A., Harris N.B.W. and Tindle A.G., Trace elements discrimination diagrams for the tectonic interpretation of granitic rocks, *Journ. Petrology.*, (25), 956-983 (1984)
22. Harris N.B.W., Pearce J.A., Tindle A.G., Geochemical characteristics of collision-zone magmatism, *Journ. Geol. Soc., London, Special Pub.* (19), 67-81 (1968)
23. Whalen J.B., Currie K.L., Chappell B.W., A-type granites: Geochemical characteristics, discrimination and petrogenesis, *Contr. Min. Petrology*, (95), 407-419 (1987)
24. Hasken L.A., Haskin M.A., Frey F.A., Wildman T.R., Relative and absolute terrestrial abundances of the rare earths. In: Ahrens L.H. (ed.) Origin and distribution of the elements. Pergamon, Oxford, pp. 889-911 (1968)
25. Masuda A., Nakamura N., Tanaka T., Fine structure of mutually normalised rare-earth patterns of chondrites, *Geochim. et Cosmochim. Acta*, (37), 239-248 (1973)

26. Weaver B., Tarney J., Empirical approach to estimating the composition of the continental crust, *Nature*, (310) 575-577 (1984)
27. Clarke D.B., Two centuries after Hutton's Theory of the Earth: the status of granite science, *Transaction Royal Soc. Edinburg Earth Sci.*, (87), 353-359 (1996)
28. Pearce J.A., Sources and settings of granitic rocks. *Episode*, (9), 120-125 (1996)
29. Chappell B.W. and White A.J.R., Two contrasting granite types, *Pacific Geol.*, (8), 173-174 (1974)
30. Tindle A.G. and Pearce J.A., Assimilation and partial melting of continental crust: evidence from the mineralogy and geochemistry of autoliths and xenoliths, *Lithos.*, (16), 185-202 (1983)
31. Nagasawa H., Schnetzler C.C., Partitioning of rare earth, alkali and alkaline elements between phenocrysts and acidic igneous magma, *Geochim. et Cosmochim. Acta.*, (35), 953-968 (1971)
32. Hanson G.N., The implications of trace elements to the petrogenesis of igneous rocks of granitic composition, *Earth Planetary Sci. Lett.*, (38), 26-43 (1978)
33. Abdel-Rahman A.M., Petrogenesis of early-orogenic diorites, tonalities and post-orogenic trondjemites in the Nubian Shield, *Journal Petrology*, (31), 1285-1312 (1990)
34. Harris N.B.W., Ayres M., Massey J., The incongruent melting of muscovite: Implications for the geochemistry and extraction of granite magma, *Journ. Geophysics Research*, (100), 15777-15787 (1995)
35. Mittlefehldt D.W. and Miller C.F., Geochemistry of the Sweet-water Wash pluton, California: implications for 'anomalous' trace element behaviour during differentiation of felsic magmas, *Geochim. et Cosmochim. Acta*, (47), 109-124 (1983)
36. Trumbull R.B., A petrological and Rb-Sr isotopic study of an early Archaean fertile granite-pegmatite system: the Sinceni Pluton in Swaziland, *Precamb. Research*, (61), 89-116 (1993)
37. Eby G.N., Chemical subdivision of the A-type granitoids: Petrogenetic and tectonic implications, *Geology*, (20), 641-644. (1992)